

Constraining Charming Penguins in Charmless B Decays

Yue-Liang Wu¹, Yu-Feng Zhou² and Ci Zhuang¹

¹*Kavli Institute for Theoretical Physics China, Institute of Theoretical Physics*

Chinese Academy of Sciences, Beijing, 100080, China

²*Korea Institute for Advanced Study, Seoul 130-722, Korea*

Abstract

We discuss the correlations of charming penguin contributions to $B \rightarrow \pi\pi$, πK and KK using approximate flavor $SU(3)$ symmetry. Strong constraints are found from the direct CP asymmetries especially in πK modes. We make a global fit to the latest data and find that only a small charming penguin is allowed, and the size of color-suppressed tree amplitude (C) relative to tree amplitudes (T) remains large $C/T \simeq 0.6$, which disfavors the possibility of a large charming penguin as an explanation for the $\pi\pi$ puzzle. We show that a small charming penguin can still have sizable effect in the time-dependence CP asymmetries in KK mode.

I. INTRODUCTION

With the successful running of the two B factories, the B physics has entered a precision era. Although the current data of hadronic B decays has show an overall agreement with the Standard Model (SM), there are a number of modes with unexpected decay rates and CP asymmetries, which are often referred to as puzzles. One of the puzzles in $\pi\pi$ modes is a large averaged branching ratio of $\pi^0\pi^0$ relative to $\pi^+\pi^-$, the current data read [1]

$$R_{\pi\pi} = \frac{2Br(\pi^0\pi^0)}{Br(\pi^+\pi^-)} = 0.51 \pm 0.08 \quad (1)$$

which is significantly larger than theoretical estimations. Another one in πK is the difference in two direct CP asymmetries

$$A_{cp}(\pi^+K^-) = -0.097 \pm 0.012, \quad A_{CP}(\pi^0K^-) = 0.050 \pm 0.025, \quad (2)$$

Both of the puzzles require a large color-suppressed tree amplitudes in flavor SU(3) topology, which is difficult to obtain from short-distance contributions. So far a satisfactory explanation is not yet available. There are other potential puzzles regarding the branching ratios and time-dependent CP asymmetries in πK mode which are relevant to the possibility of new physics. In the present work, we focus on the former ones which are more relevant to the hadronic dynamics.

It was emphasized in literature that long-distance Final State Interactions (FSIs) may play important roles in these modes [2, 3, 4], such as the inelastic rescattering channel $B \rightarrow DD_{(s)} \rightarrow \pi\pi(K), KK$ at meson level. Topologically they are equivalent to the charm-quark loops in the contractions of local operators $Q_1^c = (\bar{d}c)_{V-A}(\bar{c}b)_{V-A}$ and $Q_2^c = (\bar{d}_\alpha c_\beta)_{V-A}(\bar{c}_\beta b_\alpha)_{V-A}$ at quark level which are referred to as charming penguins[5, 6, 7]. Experimentally $Br(B \rightarrow D^+D_{(s)}^-) = [1.9 \pm 0.6(65 \pm 21)] \times 10^{-4}$ [8] are about 40(300) times larger than that of $B \rightarrow \pi^+\pi^-(K^-)$. As a consequence, a tiny OZI violating $DD \rightarrow \pi\pi$ mixing may lead to significant changes in branching ratios and CP asymmetries in $\pi\pi(\pi K)$ modes [9, 10]. A large charming penguin with an appropriate strong phase may simultaneously suppress $Br(\pi^+\pi^-)$ while enhance $Br(\pi^0\pi^0)$, thus providing a solution to the $\pi\pi$ puzzle.

The effects of charming loop have been discussed at both quark level and meson level. The situation is not yet conclusive. Estimations based on pQCD[11] and QCD sum rules [12] favor

a small size. While in the framework of Soft Collinear Effective Theory (SCET) the charming penguin could be large, depending on the jet function[13]. The meson level calculations using effective Lagrangian for mesons favor a large charming penguin comparable to QCD penguin in πK [14, 15, 16, 17]. But the patterns in $\pi\pi$ data can not be well reproduced [16].

Note that a global analysis using approximate flavor SU(3) symmetry for all the $\pi\pi$, πK and KK modes may provide a powerful constraint on charming penguins. This is because the presence of charming penguin not only modifies the individual decay amplitude but also changes the correlations among them, which has not been enough emphasized in previous analysis. The correlations are of particular importance in distinguishing charming penguin from QCD penguin. First, although the two type of amplitudes always appear together, in $\Delta S = 1$ modes they are both nearly real, but in $\Delta S = 0$ modes they differ by a phase angle β of the unitarity triangle. The correlations in the predictions of direct CP asymmetries are changed. Second, the $\Delta S = 1$, $B \rightarrow \pi K$ modes are penguin-dominant, which constrain the absolute size of charming penguin together with QCD penguin, while the $\Delta S = 0$, $B \rightarrow \pi\pi$ modes are tree-dominant and more sensitive to the tree-penguin interference. A strong constraint comes when they are combined together. Finally, the $\Delta S = 0$, $B \rightarrow KK$ modes provides a testing ground for the charming penguin. In the SM, the time-dependent CP asymmetry $S(K_S K_S)$ is nearly zero because only QCD penguin contributes. The presence of charming penguin provides an additional amplitude with different weak and strong phases. Thus a significant deviation from zero is possible.

The present work is organized as follows. In section II, we discuss the nontrivial correlations caused by long-distance charming penguin using the QCD factorization results for short-distance contributions. In section III, we make a largely model-independent global determination for the charming penguin using the latest data. The results show that a small charming penguin is favored, which can not play any significant role in resolving the $\pi\pi$ puzzle. But it can still significantly affect the prediction for $S(K_S K_S)$. Some remarks and conclusions are in section IV.

II. CHARMING PENGUIN CONTRIBUTION TO INDIVIDUAL MODES

The simplest way to see the correlated contributions from charming penguins in different modes is to fix other hadronic amplitudes to their theoretical values. To this end, we

decompose the whole decay amplitudes (\mathcal{A}) into short-distance (\mathcal{A}_{SD}) and long-distance (\mathcal{A}_{SL}) part $\mathcal{A} = \mathcal{A}_{SD} + \mathcal{A}_{LD}$, and take the short-distance part from theoretical calculations. The long-distance part is assumed to be dominated by charming penguins. The decay amplitudes are related to the observable of decay branching ratio and direct CP asymmetry as follows

$$Br = \frac{p_c \tau_B}{16\pi m_B^2} (|\mathcal{A}|^2 + |\bar{\mathcal{A}}|^2), \quad a_{cp} = \frac{|\bar{\mathcal{A}}|^2 - |\mathcal{A}|^2}{|\bar{\mathcal{A}}|^2 + |\mathcal{A}|^2}, \quad (3)$$

where p_c is the momentum of final state meson in the B meson rest frame and $\tau_B = 1.530(1.638) \times 10^{-12}s$ [8] is the neutral (charged) B meson life-time. The time dependent CP asymmetry is

$$\begin{aligned} a_{cp}(t) &= \frac{\Gamma(\bar{B}^0 \rightarrow f_{CP}) - \Gamma(B^0 \rightarrow f_{CP})}{\Gamma(\bar{B}^0 \rightarrow f_{CP}) + \Gamma(B^0 \rightarrow f_{CP})} \\ &= S \cdot \sin(\Delta m_B \cdot t) - C \cdot \cos(\Delta m_B \cdot t). \end{aligned} \quad (4)$$

The definition of quantities S and C are given by

$$S = \text{Im} \left(\frac{q}{p} \frac{\bar{\mathcal{A}}}{\mathcal{A}} \right), \quad C = \frac{|\mathcal{A}|^2 - |\bar{\mathcal{A}}|^2}{|\bar{\mathcal{A}}|^2 + |\mathcal{A}|^2} = -a_{cp}, \quad (5)$$

where $(q/p) = e^{-2i\beta}$ in the SM with β one of the angles of the unitarity triangle (UT). In what follows we take the CKM matrix elements V_{ub} and V_{cb} from the global CKM fits [18]

$$V_{ub} = (3.57 \pm 0.17) \times 10^{-3}, \quad V_{cb} = 0.0405^{+0.0032}_{-0.0029}. \quad (6)$$

To fix the profile of the UT we also use the best fitted value of [18]

$$\gamma = 1.170^{+0.048}_{-0.079}, \quad (7)$$

which corresponds to a best fitted $\beta = 0.379 \pm 0.017$.

Recently the theoretical calculations for hadronic matrix elements have been improved to next to leading α_s^2 order (NLO) in the framework of QCD factorization [19, 20] and perturbative QCD (pQCD) [11, 21]. In QCD factorization approach, the hard spectator scattering effects can lift a cancellation between leading term and vertex corrections, resulting in a significant enhancement in the effective coefficient $\alpha_2(\pi\pi)$ by a factor of ~ 3 and improve the agreement with the data. Nevertheless generating a large enough spectator scattering effects still require tuning of input parameters and the latest calculation still favor a $Br(\pi^0\pi^0)$

lower than the current data. Note that in the pQCD approach, although the NLO results improve the predictions for the direct CP asymmetries in πK modes, there is no significant enhancement found in $\pi^0\pi^0$.

The whole charmless B decay amplitudes can be described by a set of flavor topological quark flavor flow diagrams [22, 23, 24, 25, 26]. In this approach the decay amplitudes are expressed in terms of diagrams such as tree (T), color-suppressed tree (C), QCD penguin (P and P_{tu}), electroweak penguin (P_{EW}), color-suppressed electroweak penguin (P_{EW}^C) etc. In the presence of charming penguin (denoted by D for $D\bar{D}$ intermediate states), the decay amplitudes for $\pi\pi$ modes are given by

$$\begin{aligned} -\bar{\mathcal{A}}(\pi^+\pi^-) &= \lambda_u(T + E - P_{tu} - P_A - \frac{2}{3}P_{EW}) - \lambda_c(P - D + P_A + \frac{2}{3}P_{EW}^C), \\ -\bar{\mathcal{A}}(\pi^0\pi^0) &= \frac{1}{\sqrt{2}}[\lambda_u(C - E + P_{tu} + P_A - P_{EW} - \frac{1}{3}P_{EW}^C) + \lambda_c(P - D + P_A - P_{EW} - \frac{1}{3}P_{EW}^C)], \\ -\bar{\mathcal{A}}(\pi^0\pi^-) &= \frac{1}{\sqrt{2}}[\lambda_u(T + C - P_{EW} - P_{EW}^C) - \lambda_c(P_{EW} + P_{EW}^C)]. \end{aligned} \quad (8)$$

The CKM factors are defined as $\lambda_q^{(s)} = V_{qd(s)}^* V_{qb}$. In general, the QCD penguin has three part $\lambda_u P_u + \lambda_c P_c + \lambda_t P_t$, which is recombined as $P_{tu} \equiv P_t - P_u$ and $P \equiv P_{tc} \equiv P_t - P_c$. The amplitudes T , C and P etc can be calculated and the typical values (in units of 10^4eV) from QCD factorization are

$$\begin{aligned} T &= A_{\pi\pi} a_{1,\pi\pi} \simeq 0.89 - 0.02i, \\ C &= A_{\pi\pi} a_{2,\pi\pi} \simeq 0.24 - 0.02i, \\ P_{tu} &= -A_{\pi\pi} (a_{4,\pi\pi}^u + r_\chi^\pi a_{6,\pi\pi}^u) \simeq 0.076 + 0.029i, \\ P &= -A_{\pi\pi} (a_{4,\pi\pi}^c + r_\chi^\pi a_{6,\pi\pi}^c) \simeq 0.084 + 0.015i, \end{aligned} \quad (9)$$

where $A_{\pi\pi} = G_F f_\pi F_0^{B \rightarrow \pi} (m_B^2 - m_\pi^2) / \sqrt{2}$. The numerical values in the above expressions are in accordance with the central values of NLO effective coefficients in QCD factorization

approach [20]

$$\begin{aligned}
\alpha_{1,\pi\pi} &= 0.975_{-0.072}^{+0.034} + (-0.017_{-0.051}^{+0.022})i, \\
\alpha_{2,\pi\pi} &= 0.275_{-0.135}^{+0.228} + (-0.024_{-0.081}^{+0.115})i, \\
\alpha_{4,\pi\pi}^u &= -0.024_{-0.002}^{+0.004} + (-0.012_{-0.002}^{+0.003})i, \\
\alpha_{4,\pi\pi}^c &= -0.028_{-0.003}^{+0.005} + (-0.006_{-0.002}^{+0.003})i, \\
r_\chi^\pi \alpha_{6,\pi\pi}^u &= -0.060_{-0.017}^{+0.001} + (-0.020_{-0.006}^{+0.005})i, \\
r_\chi^\pi \alpha_{6,\pi\pi}^c &= -0.065_{-0.019}^{+0.012} + (-0.010_{-0.004}^{+0.004})i.
\end{aligned} \tag{10}$$

The short-distance calculations suggest a t -quark dominance in QCD penguin such that $P_{tu} \simeq P$, and tiny annihilation type diagrams E, A and P_A which are power suppressed.

A. $\pi\pi$ modes

We begin with a re-examination of $\pi\pi$ puzzle in the presence of charming penguin D . In the limit of $T, C \gg P, D$, the ratio $R_{\pi\pi}$ can be expanded as follows

$$\begin{aligned}
R_{\pi\pi} &\simeq \frac{C^2}{T^2} \left[1 + 2(1 - \omega \cos \gamma) \left(\frac{P}{T} \cos(\delta_T - \delta_P) + \frac{P}{C} \cos(\delta_C - \delta_P) \right) \right. \\
&\quad \left. + 2\omega r_D \left(\frac{P}{T} \cos(\delta_T - \delta_D) + \frac{P}{C} \cos(\delta_C - \delta_D) \right) \cos \gamma \right]
\end{aligned} \tag{11}$$

where $\omega = |\lambda_c/\lambda_u| \simeq 2.73$, and $r_D \equiv D/P$ is the size of charming penguin relative to QCD penguin. It is evident that the charming penguin has opposite contributions to $\pi^+\pi^-$ and $\pi^0\pi^0$ modes. In order to enhance $R_{\pi\pi}$ one needs $\cos(\delta_C - \delta_D) > 0$ and a large r_D . In Fig. 1 we plot the ratio $R_{\pi\pi}$ as a function of r_D with different strong phases. In the numerical calculations we use the full expressions for decay rates and CP asymmetries.

It is shown in the figure that for a typically small strong phase $\delta_D = 30^\circ$, a large $2 \leq r_D \leq 2.5$ is needed to meet data of $R_{\pi\pi}$. For large strong phase $\delta_D > 90^\circ$, an even larger $r_D > 3$ is required. This confirms previous phenomenological studies in favor of large charming penguin. The direct CP asymmetric measurements provide different constraints. In the limit $T, C \gg P, D$, the direct CP asymmetries are approximated by

$$\begin{aligned}
a_{cp}(\pi^+\pi^-) &\simeq 2\omega \frac{P}{T} (\sin(\delta_T - \delta_P) - r_D \sin(\delta_T - \delta_D)) \sin \gamma, \\
a_{cp}(\pi^0\pi^0) &\simeq -2\omega \frac{P}{C} (\sin(\delta_C - \delta_P) - r_D \sin(\delta_C - \delta_D)) \sin \gamma.
\end{aligned} \tag{12}$$

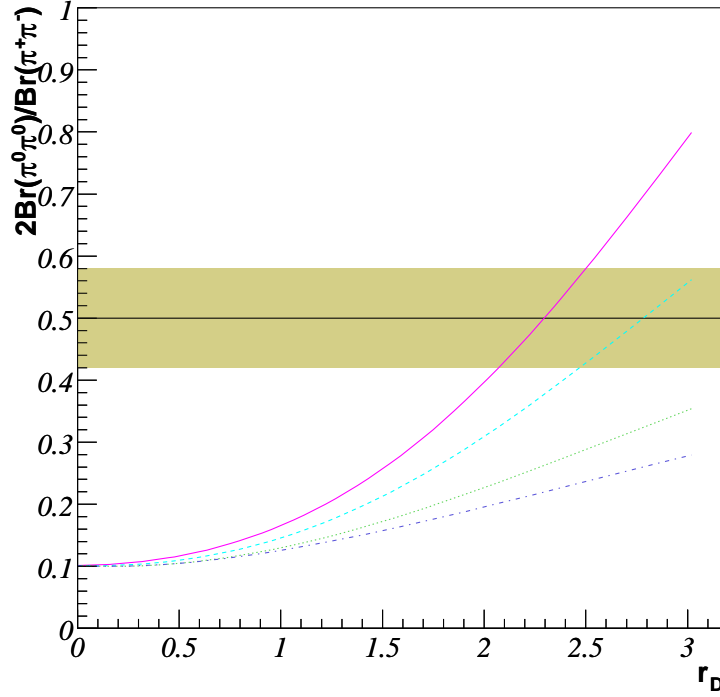


Figure 1: The ratio $R_{\pi\pi}$ as function of charming penguin. Four curves corresponds to the strong phase $\delta_D = 30^\circ$ (solid), 60° (dashed), 90° (dotted) and 120° (dot-dashed) respectively. Other parameters are default in QCD factorization estimations.

Similar to the $\pi\pi$ decay rates, the charming penguin contributions to the direct CP asymmetries are again opposite. Since δ_T and δ_C are small, roughly speaking for $0 \leq \delta_D \leq 180^\circ$, it enhances $a_{cp}(\pi^+\pi^-)$ while suppresses $a_{cp}(\pi^0\pi^0)$ to negative values. The numerical results are shown in Fig.2.

For small phase $\delta_D = 30^\circ$, the current data of $a_{cp}(\pi^+\pi^-)$ restricts the size of r_D to be $1.5 < r_D < 2$. Note that there is still a significant difference between two B factories on the measurement of $a_{cp}(\pi^+\pi^-)$ [27, 28]

$$\begin{aligned} a_{cp}(\pi^+\pi^-) &= 0.21 \pm 0.09 \pm 0.02(Babar) \\ &= 0.55 \pm 0.08 \pm 0.05(Belle) \end{aligned} \quad (13)$$

The Babar measurement favors a smaller $a_{cp}(\pi^+\pi^-)$ and the constraints on r_D is stronger. Note that the constraints on the size of r_D and the strong phase δ_D from the $a_{cp}(\pi^0\pi^0)$ and $R_{\pi\pi}$ are opposite. The preliminary data although with large uncertainty are in favor of a

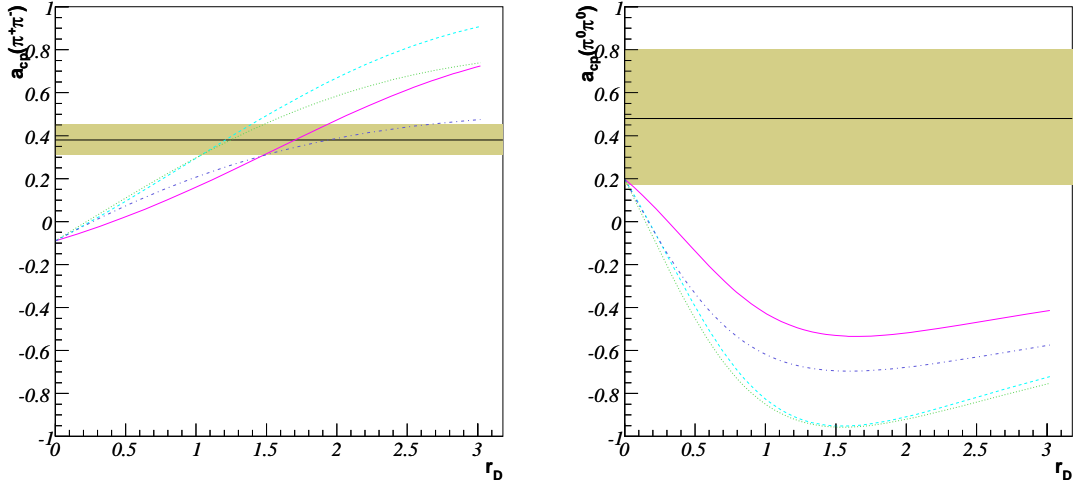


Figure 2: $a_{cp}(\pi^+\pi^-)$ and $a_{cp}(\pi^0\pi^0)$ as function of D . Four curves corresponds to the strong phase $\delta_D = 30^\circ$ (solid), 60° (dashed), 90° (dotted) and 120° (dot-dashed) respectively. Other parameters are default in QCD factorization estimations.

positive $a_{cp}(\pi^0\pi^0)$, which disfavor any large value of r_D with δ_D in the range $(0, \pi)$.

A more significant r_D dependence can be seen in the time-dependent CP asymmetries which are approximated by

$$\begin{aligned}
 S(\pi^+\pi^-) &\simeq -\sin 2(\beta + \gamma) + 2\omega \frac{P}{T} (\cos(\delta_P - \delta_T) - r_D \cos(\delta_D - \delta_T)) \sin \gamma \cos 2(\beta + \gamma), \\
 S(\pi^0\pi^0) &\simeq -\sin 2(\beta + \gamma) - 2\omega \frac{P}{C} (\cos(\delta_P - \delta_C) - r_D \cos(\delta_D - \delta_C)) \sin \gamma \cos 2(\beta + \gamma). \quad (14)
 \end{aligned}$$

Since the current global CKM fitting give a $\beta + \gamma$ close to $\pi/2$, the leading term is suppressed for both $\pi^+\pi^-$ and $\pi^0\pi^0$, which significantly enhances the charming penguin effects. As shown in Fig.3, for $\delta_D \leq 60^\circ$ the data of $S(\pi^+\pi^-)$ exclude the possibility of charm penguin since the short distance contribution is already above the experiments. The data of $S(\pi^+\pi^-)$ favors a larger strong phase δ_D . The charming penguin contribution can be either positive and negative, depending on $\cos(\delta_D - \delta_T)$. Note that in $\pi^0\pi^0$ mode the charming penguin contribution is proportional to P/C much larger than that in $\pi^+\pi^-$ which is proportional to P/T . Thus $S(\pi^0\pi^0)$ has the strongest charming penguin dependence, which can be clearly seen from Fig.3. For $\delta_D = 30^\circ$ and $r_D = 1$, the value of $S(\pi^0\pi^0)$ can be reduced to around zero. The future precision measurement of $S(\pi^0\pi^0)$ will provide a very strong constraint on r_D .

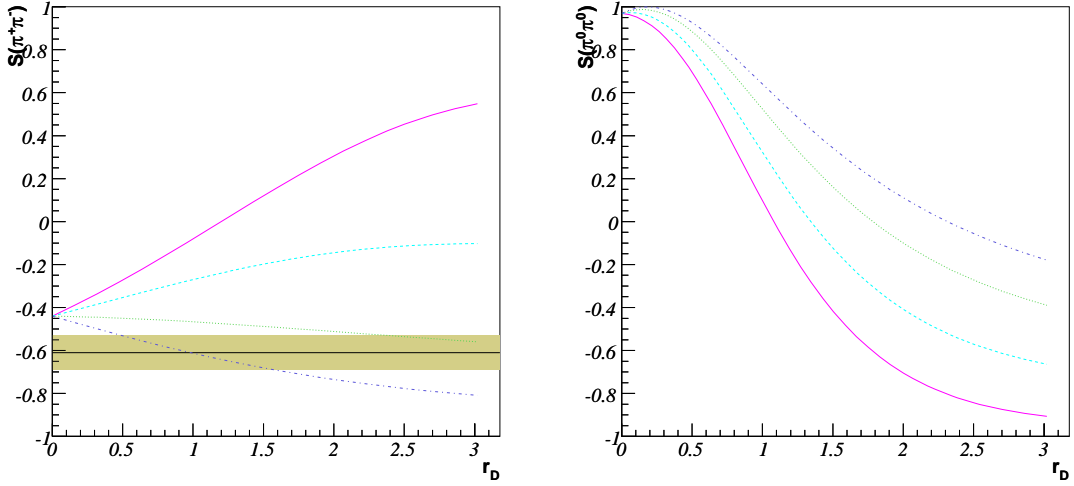


Figure 3: $S(\pi^+\pi^-)$ and $S(\pi^0\pi^0)$ as function of r_D . Four curves corresponds to the strong phase $\delta_D = 30^\circ$ (solid), 60° (dashed), 90° (dotted) and 120° (dot-dashed) respectively. Other parameters are default in QCD factorization estimations.

B. πK modes

We process to discuss the πK modes. The diagrammatic amplitudes for πK modes are given by

$$\begin{aligned}
-\bar{\mathcal{A}}(\pi^+ K^-) &= \lambda_u^s(T - P_{tu} - \frac{2}{3}P_{EW}) - \lambda_c^s(P - D + \frac{2}{3}P_{EW}^C) \\
-\bar{\mathcal{A}}(\pi^0 \bar{K}^0) &= \frac{1}{\sqrt{2}}[\lambda_u^s(C + P_{tu} - P_{EW} - \frac{1}{3}P_{EW}^C) + \lambda_c^s(P - D - P_{EW} - \frac{1}{3}P_{EW}^C)] \\
\bar{\mathcal{A}}(\pi^- \bar{K}^0) &= \lambda_u^s(A - P_{tu} + \frac{1}{3}P_{EW}^C) - \lambda_c^s(P - D - \frac{1}{3}P_{EW}^C) \\
-\bar{\mathcal{A}}(\pi^0 K^-) &= \frac{1}{\sqrt{2}}[\lambda_u(T + C + A - P_{tu} - P_{EW} - \frac{2}{3}P_{EW}^C) - \lambda_c(P - D + P_{EW} + \frac{2}{3}P_{EW}^C)]
\end{aligned} \tag{15}$$

where the amplitudes T, C and P for πK modes can be obtained by replacing $A_{\pi\pi}$ into $A_{\pi K}$. The electroweak penguin amplitude is calculated from the effective coefficients $a_{7,\pi K}$ and $a_{9,\pi K}$

$$\begin{aligned}
P_{EW} &= \frac{3}{2}A_{\pi K}(a_{7,\pi K}^c - a_{9,\pi K}^c) \simeq (1.317 + 0.015i) \times 10^{-2}, \\
P_{EW,tu} &= \frac{3}{2}A_{\pi K}(a_{7,\pi K}^c - a_{9,\pi K}^c) \simeq (1.315 - 0.014i) \times 10^{-2}
\end{aligned} \tag{16}$$

which corresponds to the effective coefficients[20]

$$\begin{aligned} a_{7,\pi K}^u &= 0.058_{-0.017}^{+0.024} + (0.015_{-0.006}^{+0.010})i, \quad a_{7,\pi K}^c = 0.010_{-0.017}^{+0.011} + (0.000_{-0.006}^{+0.003})i, \\ a_{9,\pi K}^u &= -0.819_{-0.042}^{+0.080} + (0.029_{-0.023}^{+0.053})i, \quad a_{9,\pi K}^c = -0.868_{-0.026}^{+0.058} + (0.015_{-0.018}^{+0.043})i. \end{aligned} \quad (17)$$

One sees again that the t -quark dominance leads to $P_{EW} \simeq P_{EW,tu}$. In what follows we neglect the subleading color-suppressed diagram P_{EW}^C . In πK modes one can define the following two ratios for neutral and charged modes [1]

$$R_n = \frac{Br(\pi^+ K^-)}{2Br(\pi^0 \pi^0)} = 0.98 \pm 0.07, \quad R_c = \frac{2Br(\pi^0 K^-)}{Br(\pi^- \bar{K}^0)} = 1.12 \pm 0.07. \quad (18)$$

The penguin dominance leads to an estimation of $R_n \approx R_c \approx 1$. Due to a cancelation in the subleading term, $R_n \simeq R_c$ holds to a high accuracy [29, 30]. Although earlier data showed a small R_n , which is usually referred to as πK puzzle, the latest measurements show that this puzzle has been significantly reduced. It is easy to see that the dominant charming penguin contributions cancel out in both R_n and R_c and the remaining parts are suppressed by a CKM factor $\xi = |\lambda_u^s/\lambda_c^s| \simeq 0.02$

$$\begin{aligned} R_n \simeq R_c \simeq 1 - 2\xi \left[\frac{T}{P} \cos(\delta_T - \delta_P) + \frac{C}{P} \cos(\delta_C - \delta_P) - \frac{T}{P} r_D \cos(\delta_T - \delta_D) \right. \\ \left. - \frac{C}{P} r_D \cos(\delta_C - \delta_D) \right] \cos \gamma + 2 \frac{P_{EW}}{P} \cos(\delta_{P_{EW}} - \delta_P). \end{aligned} \quad (19)$$

The previous global fits without charming penguin show a remarkable agreement between theory and experiment in penguin amplitudes [31, 32, 33]. The pure penguin mode such as $\pi^- \bar{K}^0$ constrain strongly the absolute values of $|Pe^{i\delta_P} - De^{i\delta_D}|$. However, the charming penguin can still be sizable when it carries large relative strong phase. In this case, due to tiny but nonzero weak phase difference between D and P , unacceptably large CP asymmetries can be induced when the charming penguin and QCD penguin are comparable in size. The charming penguin contributions to the direct CP asymmetries in the limit $D \ll P$ are given by

$$\begin{aligned} a_{CP}(\pi^+ K^-) &\simeq -2\xi \frac{T}{P} [\sin(\delta_T - \delta_P) - r_D \sin(\delta_T - \delta_D)] \sin \gamma, \\ a_{CP}(\pi^0 \bar{K}^0) &\simeq 2\xi \frac{C}{P} [\sin(\delta_C - \delta_P) - r_D \sin(\delta_C - \delta_D)] \sin \gamma, \\ a_{CP}(\pi^- \bar{K}^0) &\simeq 2\xi r_D \sin(\delta_D - \delta_P) \sin \gamma, \\ a_{CP}(\pi^0 K^-) &\simeq -2\xi \frac{T}{P} \left[\sin(\delta_T - \delta_P) + \frac{C}{T} \sin(\delta_C - \delta_P) - r_D \sin(\delta_T - \delta_D) \right] \sin \gamma. \end{aligned} \quad (20)$$

Numerical calculations for the direct CP asymmetries are given in fig.4, which shows that when the value of P is fixed by the QCD factorization default value there is little room for D except for the unreasonable region $D \gg P$. The strongest constraint comes from $a_{cp}(\pi^+ K^-)$, for $\delta_D = 30^\circ$ the allowed value of r_D is very narrow around $r_D \simeq 0.7$. Large r_D is only allowed for some special settings such as $\delta_D = 120^\circ$. The data of $a_{cp}(\pi^0 K^-)$ imposes a similar constraint, for $\delta_D = 30^\circ$ the allowed r_D is around 0.5. For other values of the strong phase $\delta_D = 30^\circ \sim 120^\circ$ the allowed r_D is even smaller around 0.3. For the other two modes $\pi^0 \bar{K}^0$ and $\pi^- \bar{K}^0$ the constraints are much weaker due to the weakened or vanishing tree-penguin interferences. The data only disfavor the value of $r_D \sim 1$. The correlations among the four modes can be clearly seen from fig.4. The charming penguin contribution in $a_{cp}(\pi^+ K^-)$ is opposite to those in $a_{cp}(\pi^0 \bar{K}^0)$ and $a_{cp}(\pi^- \bar{K}^0)$ but similar to $a(\pi^0 K^-)$. For small δ_D and $r_D \sim 1$, $a_{cp}(\pi^+ K^-)$ and $a(\pi^0 K^-)$ reach their minimum, while $a_{cp}(\pi^0 \bar{K}^0)$ and $a_{cp}(\pi^- \bar{K}^0)$ close to their maximum.

Note that the charming penguin in $\Delta S = 1$ modes are nearly CP conserving, the time-dependent CP asymmetry for $\pi^0 K_S$ remain unchanged for small r_D

$$S(\pi^0 K_S) \simeq \sin 2\beta + 2\xi \frac{C}{P} \cos(\delta_C - \delta_P) \cos 2\beta \sin \gamma \quad (21)$$

This is due to the fact that the charming penguin contribution cancels in the ratio $\bar{\mathcal{A}}/\mathcal{A}$ at the leading order.

C. KK modes

The decay amplitudes for KK modes are given by

$$\begin{aligned} \bar{\mathcal{A}}(K^+ K^-) &= -\lambda_u(E + P_A) \\ \bar{\mathcal{A}}(K^0 \bar{K}^0) &= -\lambda_u(P_{tu} - \frac{1}{3}P_{EW}^C) - \lambda_c(P - D - \frac{1}{3}P_{EW}^C) \\ \bar{\mathcal{A}}(K^- \bar{K}^0) &= \lambda_u(A - P_{tu} + \frac{1}{3}P_{EW}^C) - \lambda_c(P - D - \frac{1}{3}P_{EW}^C) \end{aligned} \quad (22)$$

The $K^0 \bar{K}^0$ and $K^- \bar{K}^0$ are pure $\Delta S = 0$ penguin modes. The charming penguin contribution is similar to that of $\pi^- \bar{K}^0$ except for the CKM factors. From the latest data, the QCD penguin amplitudes can be extracted and found consistent with that from $\pi^- \bar{K}^0$. Note that

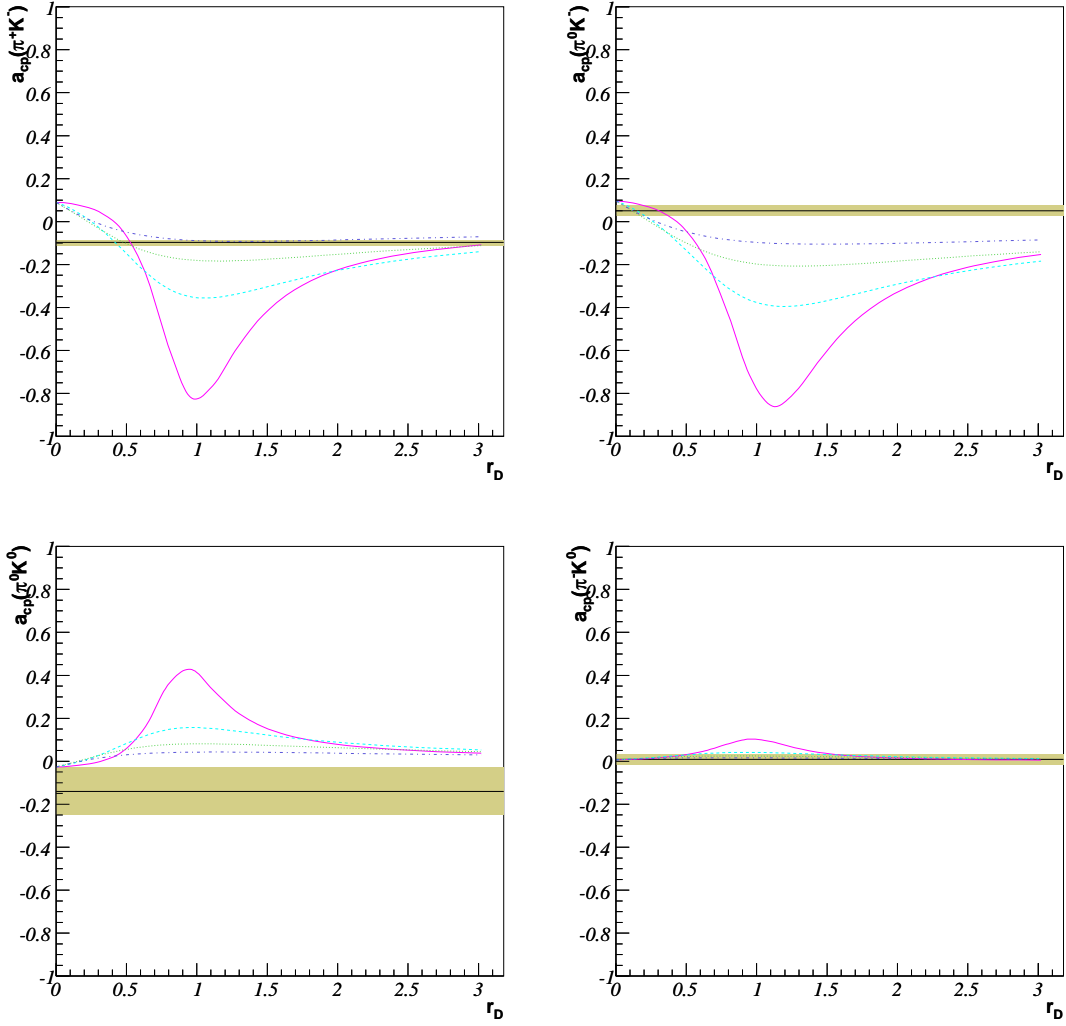


Figure 4: $a_{cp}(\pi^+ K^-)$, $a_{cp}(\pi^0 \bar{K}^0)$, $a_{cp}(\pi^- \bar{K}^0)$ and $a_{cp}(\pi^0 K^-)$ as functions of r_D . Four curves corresponds to the strong phase $\delta_D = 30^\circ$ (solid), 60° (dashed), 90° (dotted) and 120° (dot-dashed) respectively. Other parameters are default in QCD factorization estimations.

in the SU(3) limit, the direct CP asymmetry of $K^0 \bar{K}^0$ is directly linked to the $\pi^- \bar{K}^0$

$$\begin{aligned}
 a_{CP}(K^0 \bar{K}^0) &\simeq -2 \frac{\omega r_D}{\omega^2 - 2\omega \cos \gamma + 1} \sin(\delta_D - \delta_P) \sin \gamma \\
 &\simeq -\frac{\omega r_D}{\xi(\omega^2 - 2\omega \cos \gamma + 1)} a_{CP}(\pi^- \bar{K}^0)
 \end{aligned} \tag{23}$$

Note that the asymmetry is enhanced by a factor $1/\xi \simeq 50$. From the current 1σ bound $a_{CP}(\pi^- \bar{K}^0) = 0.009 \pm 0.025$, $a_{CP}(K^0 \bar{K}^0)$ can easily reach to $\mathcal{O}(-0.5)$ for $r_D \sim 0.5$. A stronger r_D dependence can be found in the time-dependent CP asymmetry of $K_S K_S$. For

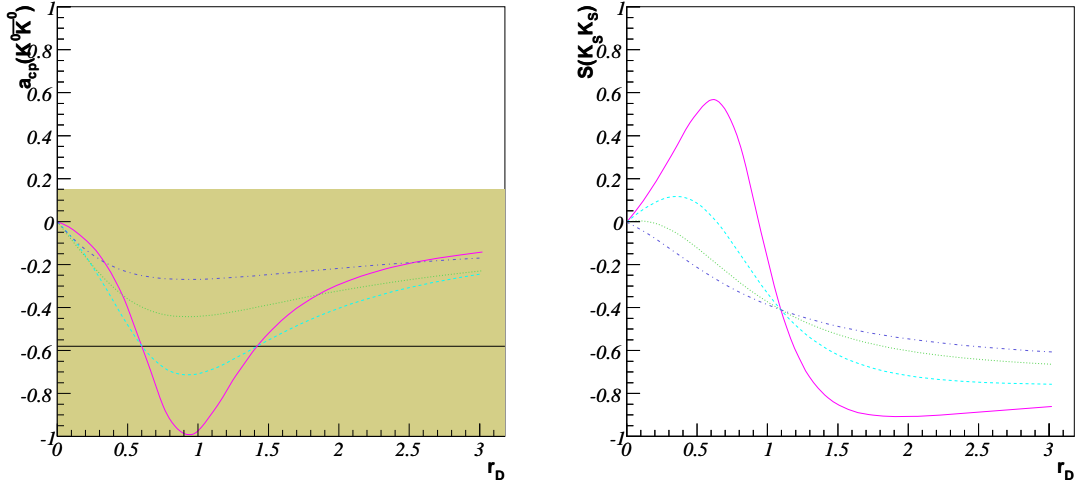


Figure 5: $a_{cp}(K^0 \bar{K}^0)$ and $S(K_S K_S)$ as function of r_D . Four curves corresponds to the strong phase $\delta_D = 30^\circ$ (solid), 60° (dashed), 90° (dotted) and 120° (dot-dashed) respectively. Other parameters are default in QCD factorization estimations.

small r_D the quantity $S(K_S K_S)$ is nonzero

$$S(K_S K_S) \simeq \frac{2\omega}{\sqrt{\omega^2 - 2\omega \cos \gamma + 1}} r_D \cos(\delta_D - \delta_P) \sin \beta. \quad (24)$$

For $r_D \sim 0.5$ and $\delta_D - \delta_P \sim 0^\circ$, the CP asymmetry can reach to be $S(K_S K_S) \sim 0.5$.

III. CONSTRAINING CHARMING PENGUINS FROM GLOBAL FIT

Let us go a step further for a model independent determination of charming penguin. Since the charming penguin and QCD penguin always come together, distinguishing the two relies on their different interference with tree type diagrams T, C and the different contributions for $\Delta S = 0$ and 1 modes. It also depends heavily on the precision of the experimental data on CP asymmetries. To isolate $SU(3)$ breaking and possible new physics effects, we shall proceed in two steps: i) Fit only to $\Delta S = 0$ modes including 11 available data points in $\pi\pi$ and KK in $SU(3)$ limit, which is a minimal set to determine the seven parameters $T, C, \delta_C, P, \delta_P, D$ and δ_D . The data for $K^+ K^-$ is excluded, because it constrains only the annihilation diagram E . The subleading P_{EW} is fixed to $T + C$ through the SM relation from the isospin analysis [24, 34, 35]. The advantages to use this data set are that the $\Delta S = 0, b \rightarrow d$ modes are expected to have less $SU(3)$ breaking and less affected

by possible new physics. The main disadvantage is that the accuracy is limited by fewer data points. ii) Fits to both $\Delta S = 0$ and 1 modes which includes 19 available data points in $\pi\pi$, KK and πK modes. Using the approximate $SU(3)$ symmetry, the fit accuracy is greatly improved. The stability of the result is checked by fit with different $SU(3)$ breaking schemes. As already mentioned, the potential puzzles in $B \rightarrow \pi\pi$ and πK modes can be divided into hadronic dynamics related and new physics related ones. Since the current data show a significant reduction of the πK puzzle in decay rates, the implication of new physics beyond the SM is mostly related to the low $S(\pi^0 K_S)$ which remains to be confirmed by future experiments. We shall exclude this data point in the fits because they have little effects in determining the charming penguin and shall discuss it separately.

There already exists a number of global fits to charmless B decays using flavor diagrammatic methods [31, 36, 37, 38, 39] and flavor $SU(3)$ invariant amplitudes [40, 41, 42], which focus on using the data as an independent determination of the weak phases in the unitarity triangle. A recent analysis [32] shows an essential agreement with the global CKM fit results on the profile of UT [18]. Since the purpose of the present work focuses on the charming penguin induced FSI, we simply take the values of V_{ub} , V_{cb} and the weak phase from the global CKM fit given in Eq.(6) and (7) as inputs to further reduce the uncertainties. In fact, it was shown in ref.[31] that the resulting weak phase γ from a model independent global fit is consistent with the standard model and insensitive to the various cases, such as the new physics effects in electroweak penguin sector, the $SU(3)$ flavor symmetry breaking effects in strong phase and the charming penguin effects. As a convention, all the B rs are in units of 10^{-6} and the phase angles are in gradient and arranged in the range of $(-\pi, +\pi)$.

A. Fit to $\pi\pi$ and KK modes

The fit to $\pi\pi$ and KK decay modes are summarized in Fit.1a(b) in Tab.II. For comparison purpose, we give in Fit.1a a determination of the leading diagrams without charming penguin amplitude. The result is characterized by a large C/T and also a slightly large P/T compared with short distance QCD factorization description

$$\frac{C}{T} = 0.63 \pm 0.09, \quad \frac{P}{T} = 0.19 \pm 0.02 \text{ (Fit.1a)}. \quad (25)$$

modes	$Br(\times 10^{-6})$	a_{CP}	S
$\pi^+\pi^-$	5.16 ± 0.22	0.38 ± 0.07	-0.61 ± 0.08
$\pi^0\pi^0$	1.31 ± 0.21	$0.48^{+0.32}_{-0.31}$	
$\pi^-\pi^0$	$5.59^{+0.41}_{-0.40}$	0.06 ± 0.05	
π^+K^-	19.4 ± 0.6	-0.097 ± 0.012	
$\pi^0\bar{K}^0(K_S)$	9.9 ± 0.6	-0.14 ± 0.11	(0.38 ± 0.19)
$\pi^-\bar{K}^0$	23.1 ± 1.0	0.009 ± 0.025	
π^0K^-	12.9 ± 0.6	0.050 ± 0.025	
K^+K^-	0.07 ± 0.12		
$K^0\bar{K}^0$	$0.96^{+0.21}_{-0.19}$	$-0.58^{+0.73}_{-0.66}$	
$K^-\bar{K}^0$	$1.36^{+0.29}_{-0.27}$	$0.12^{+0.17}_{-0.18}$	

Table I: Experimental data for charmless $\Delta S = 0$ and $\Delta S = 1$ B decay modes

In fit.1b the charming penguin contribution is switched on. One sees that there is a significant reduction of $C/T \sim 0.35$ from the best fitted central values while P/T is further enhanced. The size of D is found smaller than that of P

$$\frac{C}{T} = 0.35 \pm 0.16, \quad \frac{P}{T} = 0.36 \pm 0.19, \quad r_D = 0.63 \pm 0.62 \text{ (Fit.1b)}. \quad (26)$$

The best fits favor a constructive interference between C and P which is driven by the large decay rate of $\pi^0\pi^0$. The interference between P and D is largely destructive, which compensates the growth of P . Due to the limited degree of freedom, the inclusion of charming penguin leads to large uncertainties in all the fitted parameters. The χ^2_{min} curve for D given in Fig.6 shows a rather flat dependence of χ^2_{min} , which sets a 1σ upper bound of $r_D < 1.25$. For a meaningful determination of D , more precise data for penguin dominant πK and KK modes are needed. The prediction for the yet to be measured modes are

$$\begin{aligned} a_{cp}(\pi^0\pi^0) &= 0.29 \pm 0.48, \quad S(\pi^0\pi^0) = 0.77 \pm 0.58, \\ a_{cp}(K^0\bar{K}^0) &= 0.08 \pm 0.52, \quad S(K_SK_S) = 0.93 \pm 0.44. \end{aligned} \quad (27)$$

The predicted $a_{cp}(K^0\bar{K}^0)$ is small but $S(K_SK_S)$ is very large, which follows from the best fitted $\delta_D - \delta_P \simeq 0$ and a large $r_D = 0.62$. The uncertainties in the predictions are also large.

parameter	Fit 1a	Fit 1b	Fit 2a	Fit 2b
T	0.652 ± 0.036	$0.799^{+0.090}_{-0.151}$	0.649 ± 0.035	0.720 ± 0.111
C	0.408 ± 0.052	$0.282^{+0.115}_{-0.071}$	0.467 ± 0.044	$0.416^{+0.082}_{-0.067}$
δ_C	$-0.774^{+0.250}_{-0.212}$	$-0.983^{+0.408}_{-0.365}$	-1.096 ± 0.132	-1.189 ± 0.229
P	0.124 ± 0.010	$0.290^{+0.065}_{-0.141}$	0.124 ± 0.006	0.201 ± 0.119
δ_P	$-0.450^{+0.097}_{-0.111}$	-0.465 ± 0.115	-0.429 ± 0.052	-0.362 ± 0.116
P_{EW}	0.013 ± 0.001	0.013 ± 0.001	0.013 ± 0.001	0.013 ± 0.001
$\delta_{P_{EW}}$	-0.294 ± 0.103	-0.241 ± 0.102	-0.448 ± 0.066	-0.416 ± 0.078
D	$0(fixed)$	$0.182^{+0.080}_{-0.156}$	$0(fixed)$	0.078 ± 0.119
δ_D	$0(fixed)$	$-0.497^{+0.172}_{-0.512}$	$0(fixed)$	-0.307 ± 0.294
χ^2/dof	$4.4/6$	$3.8/4$	$15.7/12$	$15.2/10$

Table II: Hadronic parameters determined from global fit to the data. Fit.1a: fit to $\pi\pi$ and KK modes in $SU(3)$ limit without charming penguin. Fit1b: the same as Fit.1a with charming penguin included. Fit2a: fit to $\pi\pi$, πK and KK modes in $SU(3)$ limit without charming penguin. Fit2b: the same as Fit2a with charming penguin included.

B. Fit to $\pi\pi$, KK and πK modes

A stronger constraint can be obtained by including the πK modes using flavor $SU(3)$ symmetry. The $\Delta S = 1$ modes are penguin dominant, which constrains mostly the combination $P - D$, and also their relative phase from direct CP asymmetries. Although the current πK data only established the direct CP asymmetry in $\pi^+ K^-$, nontrivial bounds for other modes are already obtained. The fit with πK in $SU(3)$ limit is listed in Tab.II (Fit 2). In the case of no charming penguin (Fit.2a), one sees an even larger $C/T \simeq 0.7$ which is known to be driven by the πK CP puzzle, and the ratio P/T slightly reduced

$$\frac{C}{T} = 0.72 \pm 0.08, \quad \frac{P}{T} = 0.19 \pm 0.01 \quad (Fit.2a). \quad (28)$$

Note that the inclusion of πK modes leads to a significant reduction of the uncertainty.

The fit including the charming penguin is given in Fit.2b. Unlike the previous fits, when the πK modes are included, the ratio C/T remains large. The inclusion of charming penguin only leads to a slight reduction for C/T from ~ 0.72 to ~ 0.58 , due to the lower value of r_D

around 0.43 with an improved precision

$$\frac{C}{T} = 0.58 \pm 0.14, \quad \frac{P}{T} = 0.28 \pm 0.17, \quad r_D = 0.43^{+0.65}_{-0.43} \text{ (Fit.2b)}. \quad (29)$$

Compared with Fit.1a, the absolute size of D is reduced from 0.18 to 0.078. With the improved precision, the fit result indicates stronger constraint on r_D . This can be seen from the χ^2 curve in Fig.6. The prediction for the CP asymmetries in $\pi^0\pi^0$ and $K^0\bar{K}^0$ modes are

$$\begin{aligned} a_{cp}(\pi^0\pi^0) &= 0.53 \pm 0.15, \quad S(\pi^0\pi^0) = 0.73 \pm 0.16, \\ a_{cp}(K^0\bar{K}^0) &= -0.04 \pm 0.22, \quad S(K_SK_S) = 0.46 \pm 0.44. \end{aligned} \quad (30)$$

The reduction of $S(K_SK_S)$ is also related to the reduced r_D .

To check the SU(3) breaking effects, in Tab.III we list the fit results for two SU(3) breaking scheme: one is for SU(3) breaking in T diagrams only (Fit.3), the other one is for SU(3) breaking for both T and C (Fit.4). The SU(3) breaking factor is set to $f_K/f_\pi = 1.22$ for $\Delta S = 1$ modes. The obtained results show the value of r_D is quite stable

$$\begin{aligned} \frac{C}{T} &= 0.58 \pm 0.16, \quad \frac{P}{T} = 0.29 \pm 0.12, \quad r_D = 0.34^{+0.39}_{-0.34} \text{ (Fit.3b)} \\ \frac{C}{T} &= 0.57 \pm 0.17, \quad \frac{P}{T} = 0.29 \pm 0.13, \quad r_D = 0.31^{+0.47}_{-0.31} \text{ (Fit.4b)} \end{aligned} \quad (31)$$

The corresponding χ^2 curves are shown in Fig.6. The SU(3) breaking scheme in Fit.4b gains the lowest χ^2 , in a good agreement with previous analysis [32] on SU(3) breaking. The prediction from Fit.4.b are given by

$$\begin{aligned} a_{cp}(\pi^0\pi^0) &= 0.54 \pm 0.25, \quad S(\pi^0\pi^0) = 0.74 \pm 0.22 \\ a_{cp}(K^0\bar{K}^0) &= -0.02 \pm 0.22, \quad S(K_SK_S) = 0.38 \pm 0.19 \end{aligned} \quad (32)$$

Thus all the Fit.1-4 favor a small $a_{cp}(K^0\bar{K}^0)$ compatible with zero as a consequence of $\delta_D \simeq \delta_P$ but a positive $S(K_SK_S) = 0.3 \sim 0.4$. This kind of pattern is unique for the charming penguin contribution, which can be used to distinguish it from other contributions such as possible new physics from electroweak penguin sector. Note that the current data of $S(K_SK_S)$ are not yet conclusive. The Babar and Belle collaborations report [43, 44]

$$\begin{aligned} S(K_SK_S) &= -1.28^{+0.80+0.11}_{-0.73-0.16}, \quad C(K_SK_S) = -0.40 \pm 0.41 \pm 0.06 \text{ (Babar)} \\ S(K_SK_S) &= -0.38 \pm 0.77 \pm 0.08, \quad C(K_SK_S) = +0.38 \pm 0.38 \pm 0.05 \text{ (Belle)} \end{aligned} \quad (33)$$

parameter	Fit 3a	Fit 3b	Fit 4a	Fit 4b
T	0.651 ± 0.035	0.713 ± 0.092	0.650 ± 0.035	$0.708^{+0.077}_{-0.087}$
C	0.462 ± 0.043	$0.419^{+0.079}_{-0.063}$	0.457 ± 0.043	$0.415^{+0.081}_{-0.064}$
δ_C	-1.080 ± 0.135	-1.163 ± 0.199	-1.052 ± 0.127	-1.121 ± 0.188
P	0.124 ± 0.007	0.191 ± 0.095	0.124 ± 0.006	$0.186^{+0.076}_{-0.067}$
δ_P	-0.362 ± 0.043	-0.311 ± 0.116	-0.372 ± 0.044	-0.328 ± 0.121
P_{EW}	0.013 ± 0.001	0.013 ± 0.001	0.013 ± 0.001	0.013 ± 0.001
$\delta_{P_{EW}}$	-0.439 ± 0.066	$-0.413^{+0.073}_{-0.081}$	-0.425 ± 0.061	$-0.398^{+0.069}_{-0.081}$
D	$0(fixed)$	0.067 ± 0.095	$0(fixed)$	0.062 ± 0.100
δ_D	$0(fixed)$	-0.260 ± 0.363	$0(fixed)$	-0.295 ± 0.388
χ^2/dof	15.9/12	15.6/10	12.9/12	12.7/10

Table III: Hadronic parameters determined from global fit to $\pi\pi$, πK and KK . Fit.3a: fit without charming penguin. A $SU(3)$ breaking factor f_K/f_π is associated to tree diagrams. Fit3b: the same as Fit.3a with charming penguin included. Fit4a: fit without charming penguin. The $SU(3)$ breaking factor f_K/f_π is associated to both tree and color-suppressed tree diagrams. Fit4b: the same as Fit4a with charming penguin included.

The Babar result for $S(K_S K_S)$ favors a value outside physical region and has different sign for $C(K_S K_S)$. In the Fit.2-4, including the two free parameters D and δ_D only leads to slight reduction of the χ^2_{min} from 4.5 to 3.9 for Fit.1b (from 12.2 to 11.8 for Fit.4b). Thus the charming penguin does not play an important role to improve the agreement with the data. The best fitted C/T remains large around 0.6. The charming penguin can not play a significant role in reducing the $\pi\pi$ puzzle.

We have checked the influence of the measurement of $S(\pi^0 K_S)$. Including this piece of data leads to a big increase of the χ^2 but all the best fitted parameters remain unchanged. For instance, in the $SU(3)$ breaking scheme of Fit.4b, we get $\chi^2 = 17.7$, $C/T = 0.58 \pm 0.12$ and $r_D = 0.34^{+0.36}_{-0.34}$. As mentioned before, a low $S(\pi^0 K_S)$ can hardly be accommodated within the SM, and can be a signal of new physics. A possibility is that P_{EW} carries a large CP phase [30, 45, 46, 47]. On the other hand, the $\pi\pi$ and πK CP puzzle are more relevant to the low energy hadronic dynamics and should be investigated separately.

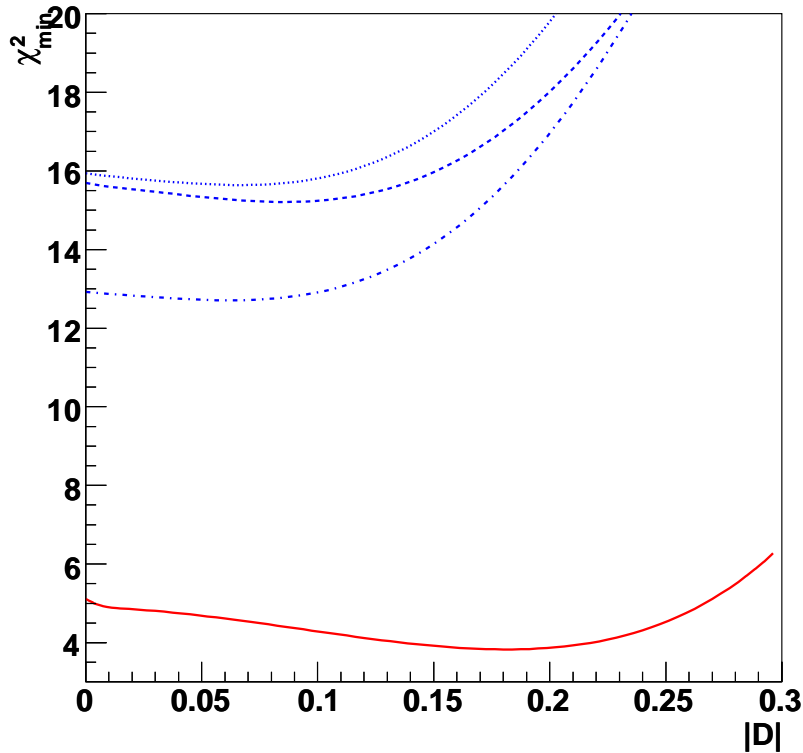


Figure 6: χ^2 as functions of D . The solid, dashed, dotted and dot-dashed curves correspond to Fit.1b, 2b, 3b and 4b respectively.

IV. DISCUSSIONS AND CONCLUSIONS

An equivalent way to see the charming penguin effects is to take P_{tu} as a free parameter not equal to P and avoiding introducing the amplitude D . A global fit including P_{tu} was done a few years ago which favored a large difference between P_{tu} and P , hence a large charming penguin was implied [36]. However, the data have been dramatically changed over the years. The main changes in the data include i) a reduced $\pi\pi$ puzzle from $R_{\pi\pi} = 0.83 \pm 0.23$ to the current value of 0.51 ± 0.08 ; ii) a reduced but more precise value of $S(\pi^+\pi^-)$ from -0.70 ± 0.30 to -0.61 ± 0.08 ; iii) a more precise $a_{cp}(\pi^+K^-)$ from -0.09 ± 0.03 to -0.097 ± 0.01 and $a_{cp}(\pi^0K^-)$ from 0.00 ± 0.12 to 0.05 ± 0.025 . The updated data are moving towards a much stronger constraints on the charming penguin. Our present conclusion is therefore different from the previous one.

In conclusion, we have found strong constraints to the charming penguins from its corre-

lated contributions to $B \rightarrow \pi\pi, \pi K$ and KK decay modes. These correlations are illustrated by adding the charming penguin amplitudes to these decay modes while assuming that other hadronic amplitudes are short-distance dominated. The charming penguin contribution has negative correlations between $Br(\pi^+\pi^-)$ and $Br(\pi^0\pi^0)$, $a_{cp}(\pi^+\pi^-)$ and $a_{cp}(\pi^0\pi^0)$, $a_{cp}(\pi^+K^-)$ and $a_{cp}(\pi^0\bar{K}^0)$ respectively. Positive correlations are found between $a_{cp}(\pi^+K^-)$ and $a_{cp}(\pi^-\bar{K}^0)$, $a_{cp}(\pi^0\bar{K}^0)$ and $a_{cp}(\pi^-\bar{K}^0)$. These correlations are unique nature of the charming penguin, and can be used to distinguish its contribution from the others. Using the latest data and assuming the approximate flavor $SU(3)$ symmetry, the size of charming penguin is constrained from a global fit. The results favor a small

$$r_D \simeq 0.3 - 0.4 \text{ and } \delta_D \simeq \delta_P.$$

which makes it unlikely as a solution to the $\pi\pi$ puzzle. The color-suppressed tree amplitude remains large $C/T \simeq 0.6$. The time-dependent CP asymmetries in $\pi^0\pi^0$ and $K_S K_S$ modes are highly sensitive to the charming penguin. We have found that charming penguin leads to a sizable $S(K_S K_S) \approx 0.3$ while keep $a_{cp}(K^0\bar{K}^0)$ compatible with zero.

Acknowledgments

We are grateful to G.Hiller for helpful discussions and early involvement of the present work. This work is supported in part by the National Science Foundation of China (NSFC) under the grant 10475105, 10491306, and the key Project of Chinese Academy of Sciences (CAS).

-
- [1] Heavy Flavor Average Group, <http://www.slac.stanford.edu/xorg/hfag/>.
 - [2] L. Wolfenstein, Phys. Rev. **D43**, 151 (1991).
 - [3] J. F. Donoghue, E. Golowich, A. A. Petrov, and J. M. Soares, Phys. Rev. Lett. **77**, 2178 (1996), hep-ph/9604283.
 - [4] M. Suzuki and L. Wolfenstein, Phys. Rev. **D60**, 074019 (1999), hep-ph/9903477.
 - [5] M. Ciuchini, E. Franco, G. Martinelli, and L. Silvestrini, Nucl. Phys. **B501**, 271 (1997), hep-ph/9703353.

- [6] C. Isola, M. Ladisa, G. Nardulli, T. N. Pham, and P. Santorelli, Phys. Rev. **D64**, 014029 (2001), hep-ph/0101118.
- [7] C. Isola, M. Ladisa, G. Nardulli, T. N. Pham, and P. Santorelli, Phys. Rev. **D65**, 094005 (2002), hep-ph/0110411.
- [8] W. M. Yao et al. (Particle Data Group), J. Phys. **G33**, 1 (2006).
- [9] S. Barshay, G. Kreyerhoff, and L. M. Sehgal, Phys. Lett. **B595**, 318 (2004), hep-ph/0405012.
- [10] S. Barshay, L. M. Sehgal, and J. van Leusen, Phys. Lett. **B591**, 97 (2004), hep-ph/0403049.
- [11] H.-n. Li and S. Mishima, Phys. Rev. **D73**, 114014 (2006), hep-ph/0602214.
- [12] A. Khodjamirian, T. Mannel, and B. Melic, Phys. Lett. **B571**, 75 (2003), hep-ph/0304179.
- [13] C. W. Bauer, D. Pirjol, I. Z. Rothstein, and I. W. Stewart, Phys. Rev. **D70**, 054015 (2004), hep-ph/0401188.
- [14] A. N. Kamal and C. W. Luo, Phys. Rev. **D57**, 4275 (1998), hep-ph/9710275.
- [15] A. N. Kamal, Phys. Rev. **D60**, 094018 (1999), hep-ph/9901342.
- [16] H.-Y. Cheng, C.-K. Chua, and A. Soni, Phys. Rev. **D71**, 014030 (2005), hep-ph/0409317.
- [17] D. Atwood and A. Soni, Phys. Rev. **D58**, 036005 (1998), hep-ph/9712287.
- [18] J. Charles et al. (CKMfitter Group), Eur. Phys. J. **C41**, 1 (2005), updated results can be find at <http://ckmfitter.in2p3.fr/>.
- [19] M. Beneke and S. Jager, Nucl. Phys. **B751**, 160 (2006), hep-ph/0512351.
- [20] M. Beneke and S. Jager, Nucl. Phys. **B768**, 51 (2007), hep-ph/0610322.
- [21] H.-n. Li, S. Mishima, and A. I. Sanda, Phys. Rev. **D72**, 114005 (2005), hep-ph/0508041.
- [22] M. Gronau, O. F. Hernandez, and London, Phys. Rev. **D52**, 6374 (1995), hep-ph/9504327.
- [23] M. Gronau, D. Pirjol, and T.-M. Yan, Phys. Rev. **D60**, 034021 (1999), hep-ph/9810482.
- [24] M. Gronau and D. Pirjol, Phys. Rev. **D62**, 077301 (2000), hep-ph/0004007.
- [25] M. Gronau and J. L. Rosner, Phys. Rev. **D66**, 053003 (2002), hep-ph/0205323.
- [26] L.-L. Chau, H.-Y. Cheng, W. K. Sze, H. Yao, and B. Tseng, Phys. Rev. **D43**, 2176 (1991).
- [27] H. Ishino et al. (Belle), Phys. Rev. Lett. **98**, 211801 (2007), hep-ex/0608035.
- [28] B. Aubert et al. (BABAR), Phys. Rev. Lett. **99**, 021603 (2007), hep-ex/0703016.
- [29] Y.-L. Wu, Y.-F. Zhou, and C. Zhuang (2006), hep-ph/0606035.
- [30] Y.-L. Wu, Y.-F. Zhou, and C. Zhuang, Phys. Rev. **D74**, 094007 (2006), hep-ph/0609006.
- [31] Y.-L. Wu and Y.-F. Zhou, Phys. Rev. **D72**, 034037 (2005), hep-ph/0503077.
- [32] C.-W. Chiang and Y.-F. Zhou, JHEP **12**, 027 (2006), hep-ph/0609128.

- [33] C.-W. Chiang and Y.-F. Zhou (2007), arXiv:0708.1612 [hep-ph].
- [34] M. Neubert, JHEP **02**, 014 (1999), hep-ph/9812396.
- [35] Y.-L. Wu and Y.-F. Zhou, Eur. Phys. J. Direct **C5**, 014 (2003), hep-ph/0210367.
- [36] C.-W. Chiang, M. Gronau, J. L. Rosner, and D. A. Suprun, Phys. Rev. **D70**, 034020 (2004), hep-ph/0404073.
- [37] Y.-L. Wu and Y.-F. Zhou, Phys. Rev. **D62**, 036007 (2000), hep-ph/0002227.
- [38] Y. F. Zhou, Y. L. Wu, J. N. Ng, and C. Q. Geng, Phys. Rev. **D63**, 054011 (2001), hep-ph/0006225.
- [39] Y.-L. Wu and Y.-F. Zhou, Phys. Rev. **D71**, 021701 (2005), hep-ph/0409221.
- [40] X. G. He et al., Phys. Rev. **D64**, 034002 (2001), hep-ph/0011337.
- [41] X.-G. He and B. H. J. McKellar (2004), hep-ph/0410098.
- [42] H.-K. Fu, X.-G. He, Y.-K. Hsiao, and J.-Q. Shi, Chin. J. Phys. **41**, 601 (2003), hep-ph/0206199.
- [43] B. Aubert et al. (BABAR), Phys. Rev. Lett. **97**, 171805 (2006), hep-ex/0608036.
- [44] K. Abe et al. (Belle) (2007), arXiv:0708.1845 [hep-ex].
- [45] T. Yoshikawa, Phys. Rev. **D68**, 054023 (2003), hep-ph/0306147.
- [46] A. J. Buras, R. Fleischer, S. Recksiegel, and F. Schwab, Phys. Rev. Lett. **92**, 101804 (2004), hep-ph/0312259.
- [47] A. J. Buras, R. Fleischer, S. Recksiegel, and F. Schwab, Acta Phys. Polon. **B36**, 2015 (2005), hep-ph/0410407.